



THE UNIVERSITY *of* EDINBURGH

Edinburgh Research Explorer

Modelling larval movement data from individual bioassays

Citation for published version:

McLellan, CR, Worton, B, Deasy, W & Birch, ANE 2015, 'Modelling larval movement data from individual bioassays' *Biometrical Journal*, vol. 57, no. 3, pp. 485-501. DOI: 10.1002/bimj.201400035

Digital Object Identifier (DOI):

[10.1002/bimj.201400035](https://doi.org/10.1002/bimj.201400035)

Link:

[Link to publication record in Edinburgh Research Explorer](#)

Document Version:

Peer reviewed version

Published In:

Biometrical Journal

Publisher Rights Statement:

© 2015 WILEY-VCH Verlag GmbH & Co. KGaA, Weinheim.

General rights

Copyright for the publications made accessible via the Edinburgh Research Explorer is retained by the author(s) and / or other copyright owners and it is a condition of accessing these publications that users recognise and abide by the legal requirements associated with these rights.

Take down policy

The University of Edinburgh has made every reasonable effort to ensure that Edinburgh Research Explorer content complies with UK legislation. If you believe that the public display of this file breaches copyright please contact openaccess@ed.ac.uk providing details, and we will remove access to the work immediately and investigate your claim.



Modelling larval movement data from individual bioassays

Chris R. McLellan¹, Bruce J. Worton^{*1}, William Deasy^{2,3}, and A. Nicholas E. Birch³

¹ School of Mathematics and Maxwell Institute for Mathematical Sciences, The University of Edinburgh, James Clerk Maxwell Building, King's Buildings, Mayfield Road, Edinburgh, EH9 3JZ, UK

² SRUC, West Mains Road, Edinburgh, EH9 3JG, UK

³ The James Hutton Institute, Invergowrie, Dundee, DD2 5DA, UK

We consider modelling the movements of larvae using individual bioassays in which data are collected at a high-frequency rate of 5 observations per second. The aim is to characterize the behaviour of the larvae when exposed to attractant and repellent compounds. Mixtures of diffusion processes, as well as Hidden Markov models, are proposed as models of larval movement. These models account for directed and localized movements, and successfully distinguish between the behaviour of larvae exposed to attractant and repellent compounds. A simulation study illustrates the advantage of using a Hidden Markov model rather than a simpler mixture model. Practical aspects of model estimation and inference are considered on extensive data collected in a study of novel approaches for the management of cabbage root fly.

Key words: Diffusion; Hidden Markov models; Mixtures; Model comparison.

Supporting Information for this article is available from the authors or on the WWW under <http://dx.doi.org/10.1022/bimj.XXXXXXX>

1 Introduction

The larva of the cabbage root fly, *Delia radicum* L. (Diptera: Anthomyiidae), is a serious pest that causes damage to *Brassica* host plants by feeding on their roots. The use of organophosphate insecticide for controlling larvae is restricted to a single pre-planting application and novel alternative treatments are currently being investigated. One of these potential treatments is to develop a way of manipulating the behaviour of the larvae in their attempts to find host plants. Studies suggest that the larvae respond to the odour of *Brassica* plants, and use the presence of specific chemicals excreted by the roots of these plants to locate suitable hosts (Ross and Anderson, 1992; Johnson and Gregory, 2006; Deasy, 2011). The larvae have also been shown to be repelled by sufficiently high concentrations of plant-specific chemicals (Finch, 1977; Košťál, 1992; Ewan, 2011). If these chemicals can be identified, and their effects upon the behaviour of the larvae understood, it may be possible to develop a control system using the appropriate plant extracts as soil amendments to act as deterrents.

Often, studies involve collecting data on locations of larvae after a given time and using standard statistical analysis of circular data, but here we consider the more challenging problem of modelling the tracks of the larvae. The former method gives only one locational observation per bioassay, whereas the number of observations obtained by the latter approach is in the thousands and thus new approaches are required to model these highly correlated data. We investigate suitable models for such data, together with appropriate methods of statistical analysis. The aim is then to use the parameters of the models as a way of summarizing the complex patterns of the tracks, and thus give a greater understanding of the behaviour of the larvae.

Bioassays were conducted at The James Hutton Institute in a research project concerned with developing novel approaches to pest management of cabbage root fly. In each bioassay, a newly hatched neonate

*Corresponding author: e-mail: Bruce.Worton@ed.ac.uk, Phone: +44 131 650 4884, Fax: +44 131 650 6553

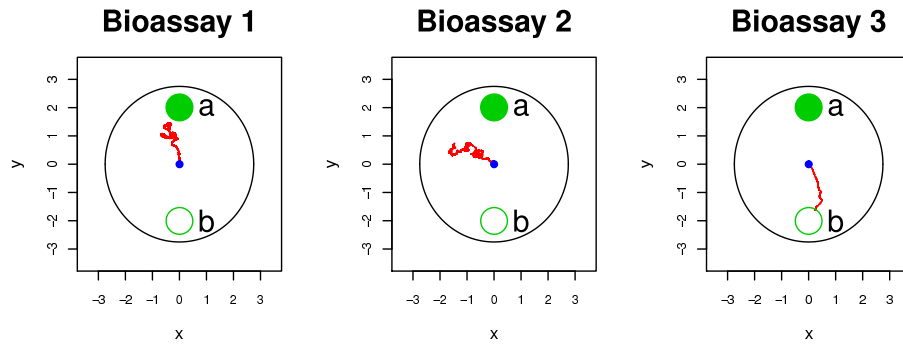


Figure 1 Tracks of cabbage root fly larvae for 3 bioassays. Each track starts at the origin (small dot) and the location of the larva is recorded every 0.2 seconds for 30 minutes using EthoVision 3.1. Each bioassay has a nominal 9000 observations. The outer circle is the arena, and the upper solid circle denoted by **a** and lower open circle denoted by **b** are the attractant (repellent for Bioassay 3) and control regions respectively.

cabbage root fly larva was placed in an arena within a 9 cm diameter Petri dish half filled with solidified agar, with a zone of host plant roots/chemical compound on one side and a no stimulus/solvent control zone on the other. The positions of the larva were then detected by infrared camera (Sanyo) and recorded using the EthoVision 3.1 software system (Noldus et al., 2001) at intervals of 0.2 seconds for 30 minutes, giving a nominal total of 9000 observations for each bioassay. However, if the larva entered one of the zones, the bioassay was terminated. Figure 1 displays plots of the tracks for 3 bioassays. In Bioassays 1–2, the upper solid circle referred to in the plots as **a** corresponds to a zone of damaged broccoli roots. As a suitable host plant, chemicals released by broccoli roots are hypothesised to act as an attractant. In Bioassay 3, **a** corresponds to a zone of allyl isothiocyanate from which the larva is repelled at the concentration tested. The lower open circle in each plot referred to as **b** is the control zone.

The subsequent sections of this article are organized as follows. In Section 2 we review the properties of a bivariate normal diffusion process for modelling the data. We propose extensions of the process by using mixture and Hidden Markov models in Section 3, with the nature of the different states chosen to account for the properties of the bioassay data. In Section 4, properties of the estimation approach for these models are explored by a simulation study. An application of the methodology to the analysis of larval movements is considered in Section 5, and the models are compared using the Bayesian Information Criterion. Finally, in Section 6, we conclude with some general remarks on the modelling.

2 Diffusion process modelling

We initially propose a model of larval movement with a general form defined by the conditional distribution of the position of the larva \mathbf{X}_{s+t} at time $s+t$ given its position \mathbf{X}_s at time s . In particular, we assume a bivariate normal distribution,

$$\mathbf{X}_{s+t}|\mathbf{X}_s \sim N\{\mathbf{a} + \mathbf{\Gamma}(\mathbf{X}_s - \mathbf{a}), \mathbf{\Phi}\}, \quad (1)$$

where \mathbf{a} is a known point of attraction or repulsion as indicated in Figure 1, and the matrices $\mathbf{\Gamma}$ and $\mathbf{\Phi}$ are defined as

$$\mathbf{\Gamma} = \begin{pmatrix} \gamma_{11} & \gamma_{12} \\ \gamma_{21} & \gamma_{22} \end{pmatrix} \quad \text{and} \quad \mathbf{\Phi} = \begin{pmatrix} \phi_{11} & \phi_{12} \\ \phi_{21} & \phi_{22} \end{pmatrix}.$$

Here, $\mathbf{\Gamma}$ is a centralization matrix determining the strength of attraction to, or repulsion from, the point \mathbf{a} , and $\mathbf{\Phi}$ is the covariance matrix of the larva's movement at each observation step. Both of these matrices are

dependent on the time t between successive observations, but as this is fixed at 0.2 seconds the parameters are constant throughout each bioassay and thus dependence on time is not explicitly included in the notation above. We note that in the modelling the observed locations of the larvae are limited to the arena within the Petri dish, as indicated in Figure 1, and if the larvae were to move outside the arena then the data collection would be terminated at the boundary of the arena.

Diffusion process (1) is similar to a bivariate Ornstein-Uhlenbeck diffusion process, which has been used in a different context to model the movements of radio tracked animals (Dunn and Gipson, 1977; Worton, 1995; Blackwell, 1997; Nations and Anderson-Sprecher, 2006). However, the latter process assumes that Γ and Φ are linked by the relation $\Phi = \Lambda - \Gamma\Lambda\Gamma^T$, where Λ is the covariance matrix of the bivariate normal equilibrium distribution of \mathbf{X}_s . In the current context, an equilibrium distribution may not exist and we therefore relax this assumption within our modelling framework.

If Γ is a diagonal matrix with positive diagonal elements, a value of γ_{11} that is less than unity indicates that the x -coordinate of the larva's position is attracted towards the x -coordinate of \mathbf{a} , while a value greater than unity implies repulsion. The parameter γ_{22} is similarly related to the y -coordinates of the larva's position and of \mathbf{a} . Having non-zero values for the non-diagonal elements of Γ introduce additional complexity, but the above statements remain roughly applicable and still give a guide to presence of attraction or repulsion provided that the non-diagonal elements are small in comparison to the diagonal elements. In the case of the larval data sets we are particularly interested in the parameter γ_{22} as attraction is associated with movement in the y direction towards \mathbf{a} from the initial starting position of the larvae.

In the bioassays, each larva is released at the origin, \mathbf{x}_0 , and generates a subsequent observed sample path, $\{\mathbf{x}_1, \dots, \mathbf{x}_n\}$, with a constant time interval between observations of 0.2 seconds. The distribution of each observation under diffusion process (1) is given by

$$\mathbf{x}_{i+1} | \mathbf{x}_i \sim N \{ \mathbf{a} + \Gamma(\mathbf{x}_i - \mathbf{a}), \Phi \}, \quad i = 0, \dots, n-1,$$

and the log likelihood for the data, up to an additive constant, is given by

$$-\frac{n}{2} \ln |\Phi| - \frac{1}{2} \sum_{i=1}^n \{ \mathbf{x}_i - \mathbf{a} - \Gamma(\mathbf{x}_{i-1} - \mathbf{a}) \}^T \Phi^{-1} \{ \mathbf{x}_i - \mathbf{a} - \Gamma(\mathbf{x}_{i-1} - \mathbf{a}) \}.$$

In simple cases such as this it is possible to obtain explicit MLEs of the parameters, but in more complex mixed processes the likelihood may be difficult to express analytically. As \mathbf{a} is known, the MLEs of the parameters of diffusion process (1) can be shown to be

$$\hat{\Gamma} = \left\{ \sum_{i=1}^n (\mathbf{x}_i - \mathbf{a})(\mathbf{x}_{i-1} - \mathbf{a})^T \right\} \left\{ \sum_{i=1}^n (\mathbf{x}_{i-1} - \mathbf{a})(\mathbf{x}_{i-1} - \mathbf{a})^T \right\}^{-1},$$

$$\hat{\Phi} = \frac{1}{n} \sum_{i=1}^n \{ \mathbf{x}_i - \mathbf{a} - \hat{\Gamma}(\mathbf{x}_{i-1} - \mathbf{a}) \} \{ \mathbf{x}_i - \mathbf{a} - \hat{\Gamma}(\mathbf{x}_{i-1} - \mathbf{a}) \}^T,$$

using a derivation similar to Anderson (1971, pp. 183–184).

While MLEs can be obtained easily for the simple diffusion process above, this is less straightforward for more complex models. Within a Bayesian framework, it is possible to obtain posterior estimates for the parameters of diffusion process (1) analytically but again this becomes extremely challenging when additional components are introduced. However, in general, Markov Chain Monte Carlo (MCMC) methods can be used to obtain posterior distributions for the parameters in such cases.

We note that the literature on statistical modelling of animal movement, which is related to the current problem, has been developed beyond (1) into much more flexible approaches (Blackwell, 2003; McClintock et al., 2012; Harris and Blackwell, 2013). However, there are some significant differences between the current type of bioassay data and wildlife tracking data. In particular, the larvae data are collected

under controlled experimental conditions and automatic monitoring is at a high-frequency collection rate of 5 locational observations per second. Each bioassay thus produces a very fine-scale track of locations to analyse and model, with thousands of observations collected over a relatively short time period of the duration of the bioassay.

3 Mixture and Hidden Markov models

3.1 Mixture modelling

We now consider a more flexible and complex model using mixtures of multiple diffusion processes. The bioassays described in Section 1 contain frequent localized movements, which occur because the position recorded for each observation is that of the larva's head, and the larvae move by expansion and contraction of their bodies. The two distinct types of movement, directed and localized, can be represented by a mixture consisting of

S1 a component related to diffusion process (1) with attraction towards (or repulsion from) \mathbf{a} ,

$$\mathbf{x}_{i+1}|\mathbf{x}_i \sim N\{\mathbf{a} + \Gamma(\mathbf{x}_i - \mathbf{a}), \Phi\},$$

and

S2 a component accounting for localized movements resulting from body contractions (without any attraction/repulsion involving \mathbf{a}),

$$\mathbf{x}_{i+1}|\mathbf{x}_i \sim N(\mathbf{x}_i, \Sigma),$$

where

$$\Sigma = \begin{pmatrix} \sigma_{11} & \sigma_{12} \\ \sigma_{21} & \sigma_{22} \end{pmatrix},$$

is a covariance matrix, with a parameter $0 < \pi < 1$ representing the probability of an observation being generated from component **S1**; for $0 \leq i \leq n - 1$.

3.2 Hidden Markov modelling

The mixture model defined in Section 3.1 assumes that the component generating each observation is independent of previous observations. This may be too much of a simplification if a larva's movement is more likely to remain in the same component than to switch. To allow for such possibilities, we consider the use of a Hidden Markov model (HMM; Frühwirth-Schnatter, 2006), which may offer a more appropriate approach for representing the behaviour of the larvae. We consider an HMM with states **S1** and **S2** as defined in Section 3.1, and a 2×2 probability transition matrix

$$\mathbf{P} = \begin{pmatrix} \pi_{11} & \pi_{12} \\ \pi_{21} & \pi_{22} \end{pmatrix},$$

where $\pi_{s_1 s_2}$ is the probability that an observation belongs to state s_2 given that the previous one belongs to state s_1 . The HMM is more computationally intensive than the simpler mixture, but can model a wider range of larval behaviour. We also consider the inclusion of further states to gain greater flexibility in our model of larval path movement.

The bioassay data sets introduced in Section 1 include many identical successive points due to the short time interval between observations. These can be represented by a third state in the HMM in which an observation is identical to the previous one,

S3 no observed movement, \mathbf{x}_{i+1} is the same as \mathbf{x}_i , and the HMM has a 3×3 transition matrix $\mathbf{P} = (\pi_{s_1 s_2})$.

To account for attraction towards (or repulsion from) the control zone \mathbf{b} in the experiment, we may include a fourth state,

S4 a diffusion process with point of attraction or repulsion \mathbf{b} , $\mathbf{x}_{i+1} | \mathbf{x}_i \sim N\{\mathbf{b} + \mathbf{\Omega}(\mathbf{x}_i - \mathbf{b}), \mathbf{\Psi}\}$, where $\mathbf{\Omega} = (\omega_{kl})$ and $\mathbf{\Psi} = (\psi_{kl})$, and in this HMM the matrix $\mathbf{P} = (\pi_{s_1 s_2})$ is 4×4 .

4 Simulation study

A simulation study was conducted to explore the properties of an estimation approach for the two-state mixture and HMM models given in Sections 3.1 and 3.2. We simulated 100 sets of 1000 observations each from the mixture model, with the following parameter values

$$\mathbf{a} = (0, 20)^T, \mathbf{\Gamma} = 0.95\mathbf{I}, \mathbf{\Phi} = 0.01\mathbf{I}, \mathbf{\Sigma} = 0.001\mathbf{I}, \pi = 0.2. \quad (2)$$

This process has one component which produces comparatively large movements influenced by the position of \mathbf{a} , and a second component consisting of smaller localized movements. We let the starting point $\mathbf{x}_0 = (0, 0)^T$ for all simulations. The two-component mixture and two-state HMM were both fitted to the simulated data sets. The following independent prior distributions were used for both of these models,

$$\gamma_{kl} \sim \text{Normal}(1, 10^2), \quad k, l = 1, 2, \quad (3)$$

$$\mathbf{\Phi} \sim \text{Inverse-Wishart}(10^{-5}\mathbf{I}, 2), \quad (4)$$

$$\mathbf{\Sigma} \sim \text{Inverse-Wishart}(10^{-5}\mathbf{I}, 2), \quad (5)$$

and represent vague prior information. The Inverse Wishart distribution is commonly used as a conjugate prior for the covariance matrix of a multivariate normal distribution (Leonard and Hsu, 1999; Gelman et al., 2003; Carlin and Louis, 2008). Further discussion of the distribution's properties can be found in Box and Tiao (1973) and Press (1982). For the mixture model, the prior distribution used for π was

$$(\pi, 1 - \pi) \sim \text{Dirichlet}\left(\frac{1}{2}, \frac{1}{2}\right), \quad (6)$$

i.e. a Beta distribution. The prior distributions used for each row $(\pi_{s_1 1}, \dots, \pi_{s_1 m})$ of the probability transition matrix \mathbf{P} for the HMMs were

$$(\pi_{s_1 1}, \dots, \pi_{s_1 m}) \sim \text{Dirichlet}\left(\frac{1}{2}, \dots, \frac{1}{2}\right), \quad s_1 = 1, \dots, m, \quad (7)$$

where m is the number of states, and in the particular case considered in the simulation study we have $m = 2$, so are using a Beta prior. Again these represent vague prior information.

Posterior distributions for the parameters were estimated with a Markov chain Monte Carlo approach using WinBUGS (Lunn et al., 2000). Summary statistics for the posterior means of selected parameters for the mixture and HMM models fitted to the simulated data sets are given in Table 1; note that the Monte Carlo errors associated with the values in the table are low relative to the values presented. These results include the mean and standard deviation, as well as the bias and root mean squared error (RMSE). The non-diagonal elements of $\mathbf{\Gamma}$, $\mathbf{\Phi}$ and $\mathbf{\Sigma}$ are close to 0 and are not displayed.

The means of the posterior means for ϕ_{11} and ϕ_{22} for the fitted two-component mixture model, displayed in Table 1, are lower than the true values, and the corresponding values for σ_{11} and σ_{22} are higher. This indicates that some observations generated by component **S1** have been assigned to component **S2** and vice versa. Note that π is estimated well, so the overall proportion of observations produced by each component has been estimated correctly. The means for γ_{11} and γ_{22} are close to the true values.

Table 1 Summary statistics of estimated posterior means of selected parameters obtained when fitting the two-component mixture model defined in Section 3.1, and the two-state HMM defined in Section 3.2, to 100 data sets of 1000 observations simulated from the two-component mixture model with the parameter values shown in (2). Presented summary statistics include the mean, standard deviation (SD), bias and root mean squared error (RMSE). The prior distributions of the parameters are given in (3), (4), (5), (6) and (7).

Parameter	Mixture				HMM			
	Mean	SD	Bias	RMSE	Mean	SD	Bias	RMSE
γ_{11}	0.9614	0.0147	0.0114	0.0186	0.9378	0.0220	-0.0122	0.0252
γ_{22}	0.9700	0.0011	0.0200	0.0200	0.9528	0.0015	0.0028	0.0032
ϕ_{11}	0.0064	0.0007	-0.0036	0.0037	0.0095	0.0010	-0.0005	0.0011
ϕ_{22}	0.0065	0.0007	-0.0035	0.0036	0.0095	0.0010	-0.0005	0.0011
σ_{11}	0.0056	0.0001	0.0046	0.0047	0.0017	0.0001	0.0007	0.0007
σ_{22}	0.0034	0.0043	0.0024	0.0049	0.0006	0.0007	-0.0004	0.0008
π	0.2027	0.0021	0.0027	0.0034				
π_{11}					0.2412	0.0384	0.0412	0.0563
π_{22}					0.7616	0.0200	0.0616	0.0648

The summary statistics obtained from fitting the two-state HMM to the same simulated data sets are also presented in Table 1. As for the mixture model, the means for γ_{11} and γ_{22} are close to the true values. However, with the HMM the means for ϕ_{11} and ϕ_{22} are much closer to the true values than in the mixture model, and the same is true to a lesser extent for σ_{11} and σ_{22} . It is interesting to note that the HMM provides a satisfactory model even though the data sets were generated from a mixture model. The means for π_{11} and $\pi_{21} = 1 - \pi_{22}$ are similar, indicating that the probability that an observation is generated from state **S1** is approximately the same regardless of the state of the previous observation and correctly reflecting the true stochastic process, i.e. the fitted HMM may be viewed as being equivalent to the simpler mixture model.

We now present the results of a simulation study that was conducted involving data sets generated from an HMM. In this study, 100 data sets of 1000 observations were simulated from the two-state HMM defined in Section 3.2, with parameter values

$$\mathbf{a} = (0, 20)^T, \mathbf{\Gamma} = 0.95\mathbf{I}, \mathbf{\Phi} = 0.01\mathbf{I}, \mathbf{\Sigma} = 0.001\mathbf{I}, \pi_{11} = 0.5, \pi_{22} = 0.9, \quad (8)$$

and the two-component mixture model and two-state HMM were both fitted to the simulated data sets. Note that the value of π , the probability that an observation is generated from state **S1**, is equal to 1/6 as given by

$$\pi = \frac{1 - \pi_{22}}{2 - \pi_{11} - \pi_{22}}. \quad (9)$$

Summary statistics for the posterior means of selected parameters of the fitted mixtures and HMMs are shown in Table 2.

The means of posterior means for γ_{11} and γ_{22} shown in Table 2 for the mixture model are close to the true values. The means for ϕ_{11} and ϕ_{22} are lower than the true values and the means for σ_{11} and σ_{22} are higher, suggesting that some observations have been assigned to the incorrect component of the mixture. The mean for π has large bias, indicating that the mixture does not adequately model data sets generated by the HMM. Clearly, the mixture model has failed to capture certain features of the HMM due to overly simplistic assumptions made by the former about switching between states. However, as we saw above, the HMM was able to model the mixture data in a satisfactory manner at the expense of some slight extra variation.

Table 2 Summary statistics of estimated posterior means of selected parameters obtained when fitting the two-component mixture model defined in Section 3.1, and the two-state HMM defined in Section 3.2, to 100 data sets of 1000 observations simulated from the two-state HMM with the parameter values shown in (8). Presented summary statistics include the mean, standard deviation (SD), bias and root mean squared error (RMSE). The prior distributions of the parameters are given in (3), (4), (5), (6) and (7).

Parameter	Mixture				HMM			
	Mean	SD	Bias	RMSE	Mean	SD	Bias	RMSE
γ_{11}	0.9560	0.0213	0.0061	0.0221	0.9429	0.0262	-0.0071	0.0271
γ_{22}	0.9660	0.0012	0.0160	0.0160	0.9578	0.0015	0.0078	0.0079
ϕ_{11}	0.0072	0.0011	-0.0028	0.0030	0.0087	0.0014	-0.0013	0.0019
ϕ_{22}	0.0072	0.0012	-0.0028	0.0030	0.0085	0.0014	-0.0015	0.0021
σ_{11}	0.0046	0.0007	0.0036	0.0037	0.0027	0.0004	0.0017	0.0017
σ_{22}	0.0048	0.0085	0.0038	0.0093	0.0025	0.0004	0.0015	0.0016
π	0.3553	0.0191	0.1887	0.1897				
π_{11}					0.5655	0.0516	0.0655	0.0833
π_{22}					0.8764	0.0168	-0.0236	0.0289

The means of posterior means for γ_{11} and γ_{22} in Table 2 for the HMM are close to the true values, while the means for ϕ_{11} and ϕ_{22} and for σ_{11} and σ_{22} are closer to the true values than for the mixture model in Tables 1 and 2. This indicates that fewer observations are assigned to the wrong component by the HMM than by the mixture model. The means for π_{11} and π_{22} are both quite close to the true values. Overall, the results of the simulation study indicate that the fitted HMMs are similar to the true models used to generate the simulated data sets, but the mixture model approach has some limitations with regard to the flexibility of the models possible.

5 Application to larval movement data

In this section, we apply the methodology outlined in Section 3 to the larval data sets introduced in Section 1, and displayed in Figure 1. We initially use our simplest single component model from Section 2, but then consider the mixture model and HMM to account for the complex features of the data. Finally, we compare the models to assess which is the most appropriate. In the modelling we will use the priors defined in Section 4 as expert belief is vague. Use of informative prior information would be highly desirable for this problem but at the moment is difficult to specify.

5.1 Single component model

Diffusion process (1) was applied to the bioassays in Figure 1, with the prior distributions of Γ and Φ as shown in (3) and (4). Table 3 presents the summary statistics of the posterior distributions of selected parameters. The parameters γ_{12} and γ_{21} , which are not displayed, are close to 0 for all bioassays, so γ_{11} and γ_{22} describe the strength of attraction to or repulsion from \mathbf{a} in the x direction and y direction respectively. The values of γ_{12} and γ_{21} are also close to 0 for the other models used throughout Section 5. For Bioassays 1 and 2, the posterior means of γ_{11} and γ_{22} are positive but less than unity, signifying attraction towards \mathbf{a} , which is confirmed by visual inspection of Figure 1. However, the results for Bioassay 3 differ in that the posterior mean of γ_{22} is greater than unity. This corresponds to movement away from \mathbf{a} , as is evident in Figure 1.

Table 3 Summary statistics of posterior distributions of selected parameters for diffusion process (1) for Bioassays 1–3. The prior distributions of Γ and Φ are as given in (3) and (4).

	Parameter	Posterior summary statistics				
		Mean	Median	SD	2.5%	97.5%
Bioassay 1	γ_{11}	0.9996	0.9996	0.0003	0.9991	1.0001
	γ_{22}	0.9997	0.9997	0.0001	0.9996	0.9999
	ϕ_{11}^\dagger	4.2576	4.2567	0.0641	4.1354	4.3882
	ϕ_{22}^\dagger	4.5144	4.5142	0.0668	4.3875	4.6448
Bioassay 2	γ_{11}	0.9999	0.9999	0.0001	0.9997	1.0002
	γ_{22}	0.9999	0.9999	0.0001	0.9998	1.0001
	ϕ_{11}^\dagger	4.1360	4.1350	0.0623	4.0174	4.2629
	ϕ_{22}^\dagger	3.9608	3.9608	0.0586	3.8481	4.0774
Bioassay 3	γ_{11}	0.9994	0.9994	0.0020	0.9957	1.0035
	γ_{22}	1.0002	1.0002	0.0005	0.9993	1.0011
	ϕ_{11}^\dagger	3.4986	3.4916	0.1466	3.2313	3.8028
	ϕ_{22}^\dagger	5.2357	5.2284	0.2189	4.8198	5.6868

† Values multiplied by 10^5 .

5.2 Mixture model

The mixture model described in Section 3.1 was applied to the bioassays, and selected results of the analysis are presented in Table 4. For Bioassays 1 and 2, the posterior means of σ_{11} and σ_{22} are five orders of magnitude smaller than those for ϕ_{11} and ϕ_{22} . This means that component **S2** of the mixture has captured the localized movements of the larva, while state **S1** represents larger directed movements. For both of these bioassays, about 20% of movements are assigned to component **S1**, and the posterior means of γ_{11} and γ_{22} are positive but less than unity, indicating attraction towards **a**. For Bioassay 3, the posterior means of ϕ_{11} , ϕ_{22} , σ_{11} and σ_{22} indicate that component **S1** consists of the larva's larger directed movements while state **S2** has accounted for localized movements. However, the posterior mean of γ_{22} is greater than unity, and this is consistent with the path in Figure 1, which shows movement away from **a**.

5.3 Hidden Markov models

The two-state HMM described in Section 3.2 was applied to the bioassays, as it contains desirable features of attraction to (or repulsion from) the point **a** as well as allowing for localized movements due to body contraction, but also has the transition matrix **P**. Summary statistics for selected parameters are displayed in Table 5, and describe a process with some differences from the mixture. For Bioassay 1, the posterior means of π_{11} and π_{22} suggest that the larva spends about 13% of the time in state **S1** as given by (9), considerably less than the 23% obtained for the mixture model. The posterior means of γ_{11} and γ_{22} indicate attraction towards **a**, in the y direction. However, the smaller proportion of movements assigned to state **S1** means that this influence is weaker than suggested by the mixture model. For Bioassays 2 and 3, the results are similar to those obtained for the mixture, in that the posterior means show attraction towards **a** for Bioassay 2 and repulsion for Bioassay 3, and the larva spends approximately 22% and 25% of the time in state **S1** respectively for these two bioassays.

The three-state model was fitted to each of the bioassays to investigate whether a third state **S3** might improve on possible inadequacies of the two-state HMM by incorporating a null move state into the HMM. For Bioassays 1 and 2, as shown in Tables 6 and 7 respectively, the posterior means of γ_{11} and γ_{22} again imply attraction towards **a**. The posterior means of σ_{11} and σ_{22} reveal that state **S2** consists almost entirely

Table 4 Summary statistics of posterior distributions of selected parameters for the two-component mixture model defined in Section 3.1 for Bioassays 1–3. The prior distributions of the parameters are given in (3), (4), (5) and (6).

	Parameter	Posterior summary statistics				
		Mean	Median	SD	2.5%	97.5%
Bioassay 1	γ_{11}	0.9984	0.9984	0.0012	0.9959	1.0007
	γ_{22}	0.9990	0.9990	0.0003	0.9983	0.9997
	ϕ_{11}^{\dagger}	1.8312	1.8303	0.0558	1.7280	1.9414
	ϕ_{22}^{\dagger}	1.9346	1.9344	0.0618	1.8135	2.0602
	σ_{11}^{\ddagger}	0.1449	0.1449	0.0025	0.1402	0.1496
	σ_{22}^{\ddagger}	0.1447	0.1447	0.0025	0.1399	0.1498
	π	0.2328	0.2328	0.0045	0.2237	0.2417
	Bioassay 2	γ_{11}	0.9993	0.9993	0.0006	0.9980
γ_{22}		0.9994	0.9994	0.0004	0.9986	1.0002
ϕ_{11}^{\dagger}		1.9181	1.9161	0.0622	1.8007	2.0436
ϕ_{22}^{\dagger}		1.8430	1.8432	0.0577	1.7305	1.9598
σ_{11}^{\ddagger}		0.1416	0.1416	0.0024	0.1370	0.1463
σ_{22}^{\ddagger}		0.1417	0.1417	0.0025	0.1368	0.1465
π		0.2150	0.2151	0.0044	0.2059	0.2234
Bioassay 3		γ_{11}	0.9986	0.9987	0.0081	0.9833
	γ_{22}	1.0011	1.0012	0.0018	0.9974	1.0043
	ϕ_{11}^{\dagger}	1.3869	1.3834	0.1121	1.1851	1.6284
	ϕ_{22}^{\dagger}	1.8642	1.8524	0.1547	1.5812	2.1985
	σ_{11}^{\ddagger}	1.1583	1.1575	0.0548	1.0549	1.2697
	σ_{22}^{\ddagger}	1.1555	1.1537	0.0566	1.0435	1.2677
	π	0.2535	0.2535	0.0127	0.2294	0.2785

\dagger Values multiplied by 10^4 .

\ddagger Values multiplied by 10^8 .

of movement in the y direction, as σ_{22} is several orders of magnitude larger than σ_{11} . The posterior means of ϕ_{11} and ϕ_{22} are of roughly the same order of magnitude as that of σ_{22} , implying that the model consists of two components with movements in the y direction of the same order of magnitude plus the “null” state **S3** of stationary observations, whereas the mixture model and two-state HMM only suggested one diffusion process consisting of larger movements and the other of much smaller movements. This difference may be interpreted as stationary observations that were assigned to one of the two diffusion processes by the two-state model instead being assigned to the null state **S3** by the three-state model. Therefore, the three-state HMM with account taken for lack of movement at certain steps, appears to provide a more satisfactory description of the observed data.

Table 5 Summary statistics of posterior distributions of selected parameters for the two-state HMM defined in Section 3.2 for Bioassays 1–3. The prior distributions of the parameters are given in (3), (4), (5) and (7).

	Parameter	Posterior summary statistics				
		Mean	Median	SD	2.5%	97.5%
Bioassay 1	γ_{11}	1.0001	1.0001	0.0008	0.9985	1.0018
	γ_{22}	0.9983	0.9983	0.0006	0.9971	0.9995
	ϕ_{11}^{\dagger}	0.5118	0.5111	0.0213	0.4707	0.5535
	ϕ_{22}^{\dagger}	3.4438	3.4421	0.1408	3.1675	3.7268
	σ_{11}^{\ddagger}	0.4131	0.4131	0.0064	0.4012	0.4253
	σ_{22}^{\ddagger}	0.1279	0.1279	0.0020	0.1238	0.1320
	π_{11}	0.3929	0.3926	0.0143	0.3647	0.4208
	π_{22}	0.9090	0.9090	0.0033	0.9023	0.9154
Bioassay 2	γ_{11}	0.9993	0.9994	0.0006	0.9981	1.0006
	γ_{22}	0.9995	0.9994	0.0004	0.9986	1.0004
	ϕ_{11}^{\dagger}	1.9170	1.9146	0.0616	1.8000	2.0420
	ϕ_{22}^{\dagger}	1.8445	1.8421	0.0593	1.7306	1.9660
	σ_{11}^{\ddagger}	0.1416	0.1416	0.0024	0.1370	0.1462
	σ_{22}^{\ddagger}	0.1415	0.1415	0.0024	0.1369	0.1462
	π_{11}	0.3916	0.3914	0.0110	0.3707	0.4127
	π_{22}	0.8332	0.8331	0.0043	0.8248	0.8419
Bioassay 3	γ_{11}	0.9993	0.9995	0.0070	0.9849	1.0155
	γ_{22}	1.0013	1.0012	0.0014	0.9985	1.0042
	ϕ_{11}^{\dagger}	1.3869	1.3791	0.1184	1.1747	1.6289
	ϕ_{22}^{\dagger}	1.8557	1.8460	0.1488	1.5898	2.1567
	σ_{11}^{\ddagger}	1.1553	1.1557	0.0543	1.0493	1.2636
	σ_{22}^{\ddagger}	1.1539	1.1519	0.0568	1.0463	1.2763
	π_{11}	0.4439	0.4444	0.0285	0.3888	0.4999
	π_{22}	0.8108	0.8107	0.0129	0.7842	0.8351

\dagger Values multiplied by 10^4 .

\ddagger Values multiplied by 10^8 .

Table 6 Summary statistics of posterior distributions of selected parameters for the three-state HMM defined in Section 3.2 for Bioassay 1. The prior distributions of the parameters are given in (3), (4), (5) and (7).

Parameter	Posterior summary statistics				
	Mean	Median	SD	2.5%	97.5%
γ_{11}	0.9966	0.9966	0.0023	0.9921	1.0011
γ_{22}	0.9996	0.9996	0.0003	0.9991	1.0001
ϕ_{11}^{\dagger}	3.5111	3.5086	0.1502	3.2375	3.8238
ϕ_{22}^{\dagger}	0.5403	0.5400	0.0236	0.4961	0.5881
σ_{11}^{\ddagger}	0.9978	0.9964	0.0448	0.9145	1.0887
σ_{22}^{\ddagger}	3.4700	3.4679	0.1526	3.1766	3.7815
π_{11}	0.4112	0.4107	0.0149	0.3828	0.4407
π_{12}	0.0691	0.0688	0.0077	0.0548	0.0842
π_{13}	0.5197	0.5198	0.0149	0.4902	0.5486
π_{21}	0.0618	0.0616	0.0077	0.0476	0.0774
π_{22}	0.3704	0.3701	0.0152	0.3416	0.4006
π_{23}	0.5678	0.5675	0.0157	0.5363	0.5978
π_{31}	0.0843	0.0843	0.0033	0.0777	0.0908
π_{32}	0.0808	0.0808	0.0034	0.0743	0.0879
π_{33}	0.8349	0.8349	0.0045	0.8260	0.8437

\dagger Values multiplied by 10^4 .

\ddagger Values multiplied by 10^8 .

Table 7 Summary statistics of posterior distributions of selected parameters for the three-state HMM defined in Section 3.2 for Bioassay 2. The prior distributions of the parameters are given in (3), (4), (5) and (7).

Parameter	Posterior summary statistics				
	Mean	Median	SD	2.5%	97.5%
γ_{11}	0.9986	0.9985	0.0012	0.9963	1.0009
γ_{22}	0.9998	0.9998	0.0003	0.9992	1.0004
ϕ_{11}^{\dagger}	3.4403	3.4376	0.1502	3.1513	3.7494
ϕ_{22}^{\dagger}	0.5810	0.5805	0.0254	0.5335	0.6334
σ_{11}^{\ddagger}	0.1167	0.1165	0.0057	0.1063	0.1284
σ_{22}^{\ddagger}	3.4241	3.4196	0.1661	3.1162	3.7734
π_{11}	0.2855	0.2858	0.0139	0.2588	0.3124
π_{12}	0.1008	0.1003	0.0092	0.0840	0.1196
π_{13}	0.6137	0.6136	0.0147	0.5848	0.6431
π_{21}	0.1271	0.1268	0.0116	0.1052	0.1509
π_{22}	0.2710	0.2711	0.0154	0.2413	0.3007
π_{23}	0.6019	0.6012	0.0169	0.5694	0.6372
π_{31}	0.0936	0.0936	0.0034	0.0871	0.1001
π_{32}	0.0732	0.0732	0.0031	0.0672	0.0795
π_{33}	0.8332	0.8333	0.0044	0.8244	0.8417

\dagger Values multiplied by 10^4 .

\ddagger Values multiplied by 10^7 .

For Bioassay 3, the results, given in Table 8, are quite different from Bioassays 1 and 2. The posterior means of γ_{11} and γ_{22} imply repulsion from **a**, and the posterior means of ϕ_{11} and ϕ_{22} indicate that state **S1** consists primarily of movement in the y direction. This confirms our visual impression from Figure 1, since the larva moves almost directly away from **a**, which results in such movement. For all bioassays, the posterior means of π_{13} , π_{23} and π_{33} highlight the importance of including state **S3** in the model.

Table 8 Summary statistics of posterior distributions of selected parameters for the three-state HMM defined in Section 3.2 for Bioassay 3. The prior distributions of the parameters are given in (3), (4), (5) and (7).

Parameter	Posterior summary statistics				
	Mean	Median	SD	2.5%	97.5%
γ_{11}	1.0000	1.0000	0.0002	0.9995	1.0004
γ_{22}	1.0025	1.0025	0.0035	0.9957	1.0095
ϕ_{11}^{\ddagger}	0.6227	0.6158	0.0712	0.5014	0.7808
ϕ_{22}^{\ddagger}	2.6030	2.5861	0.2837	2.0932	3.2359
σ_{11}^{\dagger}	3.1305	3.1064	0.3911	2.4722	3.9923
σ_{22}^{\dagger}	0.8225	0.8159	0.1017	0.6442	1.0359
π_{11}	0.3308	0.3306	0.0367	0.2609	0.4053
π_{12}	0.1314	0.1299	0.0264	0.0854	0.1859
π_{13}	0.5377	0.5370	0.0389	0.4612	0.6141
π_{21}	0.0615	0.0593	0.0216	0.0260	0.1094
π_{22}	0.3623	0.3620	0.0423	0.2797	0.4491
π_{23}	0.5762	0.5760	0.0431	0.4930	0.6606
π_{31}	0.1183	0.1180	0.0110	0.0972	0.1404
π_{32}	0.0718	0.0715	0.0087	0.0553	0.0901
π_{33}	0.8100	0.8105	0.0131	0.7836	0.8353

\dagger Values multiplied by 10^4 .

\ddagger Values multiplied by 10^7 .

The four-state model was applied to the bioassays to incorporate the control zone **b** (see Figure 1) into the model, using the following independent vague priors,

$$\omega_{kl} \sim \text{Normal}(0, 10^2), \quad k, l = 1, 2,$$

$$\Psi \sim \text{Inverse-Wishart}(10^{-5}\mathbf{I}, 2),$$

with priors for the other parameters as shown in (3), (4), (5) and (7). For these fitted models the posterior means of γ_{11} and γ_{22} indicate attraction towards **a** for Bioassays 1 and 2, and repulsion for Bioassay 3, as was the case for the other models used. However, we found that the inclusion of the fourth state in the HMM added very little in terms of the feature of the behaviour in which we are primarily interested. In addition, the four-state model has a possible disadvantage that it may have some difficulty distinguishing between state **S1** and state **S4** as they can be viewed as being similar in nature, i.e. movement towards/away from the chemical/control zones in the y direction. These considerations suggest that the three-state HMM may be sufficient for our modelling.

5.4 Model comparison

The Bayesian Information Criterion (BIC) was used to give some comparison of the competing models. BIC values for the models fitted to the bioassays are presented in Table 9. The mixture and the two-state HMM are improvements over the single diffusion process. However, the three-state HMMs incorporating

null movement result in much lower BIC values for all three bioassays, and are therefore to be preferred over both two-component models. The addition of a fourth state describing influence by the control zone **b** provides further improvement over the three-state model for Bioassay 1, though the difference in BIC is not as large as the difference between the two-state and three-state models. For Bioassays 2 and 3, the three-state model is superior. The BIC values give us a guide, and together with our previous discussion above, suggest that the three-state model provides a compromise between accounting for the important features of the larval track data without incorporating unnecessary detail.

Table 9 BIC values of the various models fitted to the bioassays.

Model	Number of parameters	Bioassay		
		1	2	3
Single diffusion process	7	-129469	-130936	-16719
Two-component mixture model	11	-279611	-284020	-31864
Two-state HMM	12	-216830	-284018	-31861
Three-state HMM	16	-581770	-590949	-73338
Four-state HMM	29	-588411	-588236	-73224

5.5 Plots of posterior densities

The strength of the influence that the position of **a** has on the larva's movements is determined by $|\Gamma|$. However, as the position of **a** in each bioassay has an x -coordinate very close to the x -coordinate of the larva's starting position, the strength of attraction to or repulsion from **a** is primarily determined by the parameter γ_{22} . As noted above, a non-negative value of γ_{22} less than unity suggests movement in the direction of **a**, which corresponds to attraction, and a value greater than unity indicates repulsion. As this is the aspect of movement of primary interest, we focus our attention on the parameter γ_{22} as well as $|\Gamma|$. Posterior density plots of γ_{22} and of $|\Gamma|$ are shown in Figure 2 for the three-state HMM, and it is apparent that the majority of the densities of both parameters are below unity for Bioassays 1 and 2 and above it for Bioassay 3. Furthermore, in the case of γ_{22} the dispersion of the density obtained for Bioassay 3 is clearly different from the other two bioassays, having much higher variance. The fitted three-state models have successfully distinguished between the attraction exhibited by larvae exposed to damaged broccoli roots and repulsion from allyl isothiocyanate. The difference in variance between Bioassay 3 and the other two bioassays is less pronounced in the case of $|\Gamma|$. We note that a γ_{22} value of unity corresponds to no attraction, but not actually repulsion.

5.6 MCMC diagnostics and posterior predictive checks

Care is needed when applying MCMC techniques to ensure the simulations are providing a true picture of the posterior distribution. With all the models considered in this paper MCMC diagnostics were used to investigate any problems with model fitting. In addition, particular care is needed with mixture type problems with regard to potential 'label switching' (Stephens, 2000). Fortunately, the MCMC convergence was excellent for all models considered and also there were no issues with label switching. Figure 3 gives an illustration of the type of trace plots obtained in the MCMC in the case of the three-state HMM for the π_{11} parameter, but trace plots for the other parameters have acceptable properties. Fortunately, the structure and nature of the components (with/without attraction) are sufficiently different so that the model fitting does not lead to label switching. Note that even in models with the null state that may have potentially lead to problems, the trace plots did not show any significant issues.

With regard to sensitivity to the prior information we investigated varying the priors and found that the results were essentially unchanged unless we used very extreme changes of prior information. This may

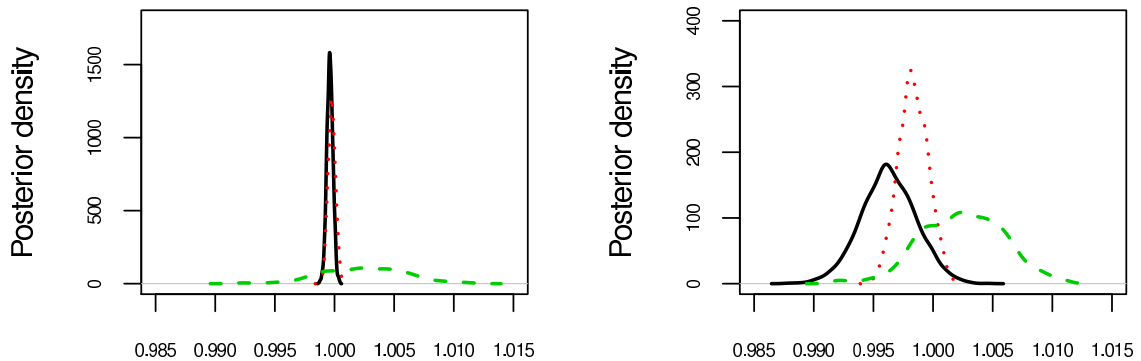


Figure 2 Posterior density plots of γ_{22} (left panel) and $|\Gamma|$ (right panel) for the three-state HMMs fitted to Bioassay 1 (solid line), Bioassay 2 (dotted line) and Bioassay 3 (dashed line).

reflect the large sample sizes involved in the analyses. As noted at the beginning of Section 5, it would be desirable to use informative prior information in the Bayesian analysis, if it were available.

Posterior predictive checks were conducted to assess the adequacy of the models (Gelman et al., 2003). Simulated tracks generated from the three-state HMM using values simulated from the posterior distribution were compared with the observed track. In particular, we used the final observation as an assessment. This is the observation that is collected in non-tracking experiments so provides a natural assessment of the adequacy of the model. Figure 4 shows the estimated posterior predictive distributions of the distance between the final location of the track and the point **a**. For Bioassay 1 the observed value is towards the lower end of the distribution, but there is no significant evidence of disagreement with the model. Similarly, for Bioassays 2 and 3, the three-state HMM seems adequate for our modelling.

6 Conclusions

We have seen that diffusion based processes may be used to model the tracks of cabbage root fly larvae. By doing this we can gain a greater understanding of the processes that govern their movements. It is clear, even from the plots of the bioassay data in Figure 1, that behaviour of the larvae in the presence of allyl isothiocyanate (Bioassay 3) is very different from that in the case of damaged broccoli roots (Bioassays 1 and 2), but we can use the modelling to characterize the movements more quantitatively. The mixture of bivariate normal diffusion processes successfully indicates that the larvae in Bioassays 1 and 2 are moving towards the zone of damaged broccoli roots, and that the larva in Bioassay 3 is repelled from the allyl isothiocyanate. However, we found that there are advantages of using an HMM approach, and due to their increased complexity the HMMs produced more biologically realistic descriptions.

Although it is possible to collect extensive sets of data with the currently available experimental equipment and software, care is needed to incorporate important features of the movement into our models of larvae paths. The two-state HMM captures the salient features of the data and clearly differentiates between the attraction towards **a** present in Bioassays 1 and 2 and the repulsion in Bioassay 3. The addition of a third “null” state, representing no movement, results in a more appropriate model that accounts for the successive identical observations present in the data. Model comparison using BIC indicates that the three-state model is far superior to the two-state HMM and mixture, and it is also preferred to the four-state model for two of three bioassays.

While the models used here are successful at identifying attraction to and repulsion from **a** and provide a suitable model for the bioassays, we conclude the article by considering possible alternatives and refinements. Further improvement to the models might involve modification to include more pronounced directional persistence. The data plot for Bioassay 3 in particular, presented in Figure 1, suggests that the

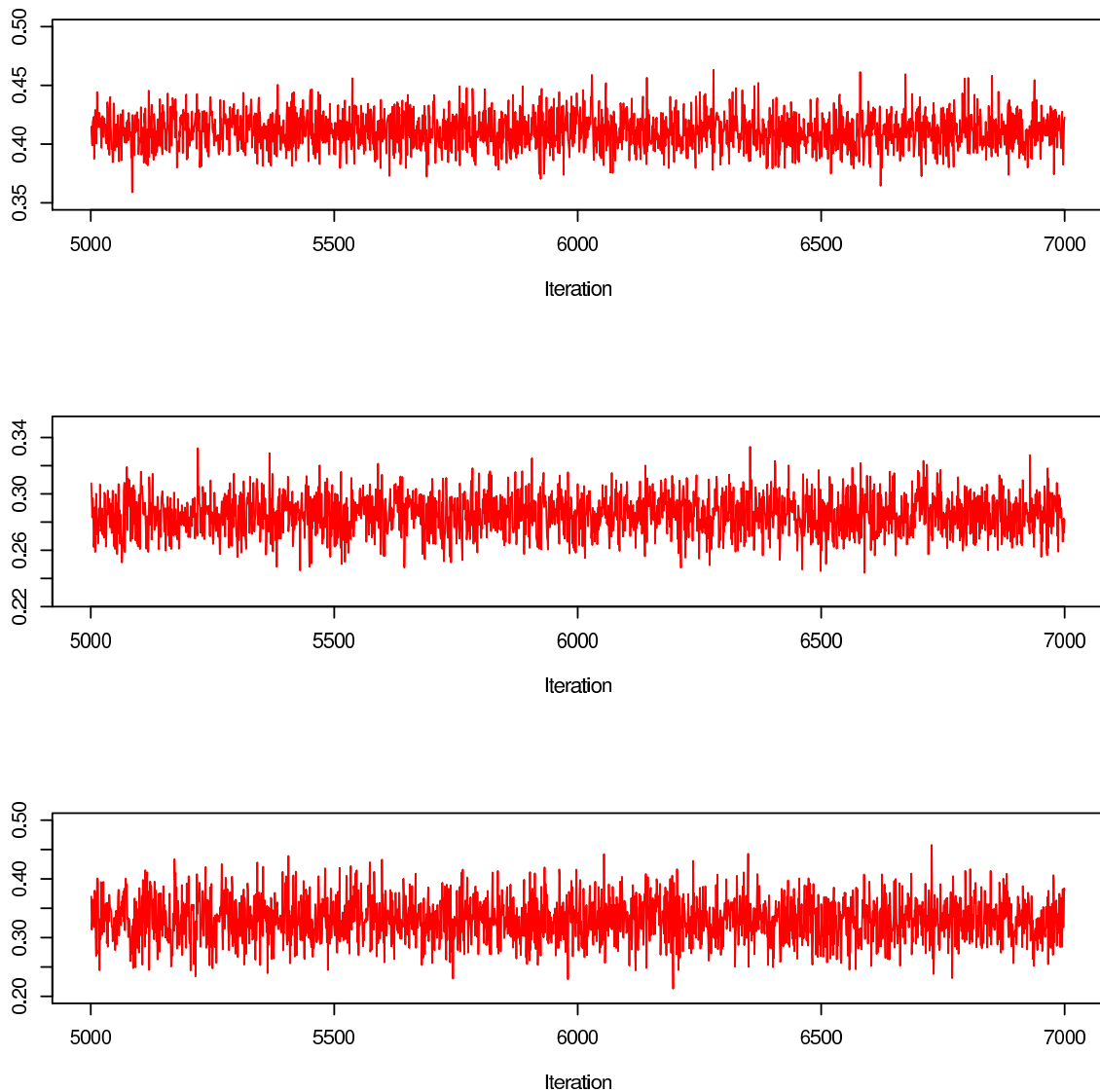


Figure 3 MCMC trace plots for the parameter π_{11} for the three-state HMMs: Bioassay 1 (upper panel), Bioassay 2 (middle panel) and Bioassay 3 (lower panel).

movements of the larva are highly dependent on the current direction of movement, whereas the HMM used here only involves first-order dependence and so is fairly limited in its ability to model this behaviour. As such, a natural development would be to incorporate higher-order dependence. This may result in models even more appropriate for the bioassay data, and allow further inference to be made about the behaviour of the larvae. Nevertheless, the models we consider in this paper have worked well in extracting important behavioural responses with regard to the study of novel approaches for the management of cabbage root fly.

In this paper we have investigated modelling a small number of tracks from individual bioassays so that although the number of observations per bioassay is very large the sample size in terms of tracks is very

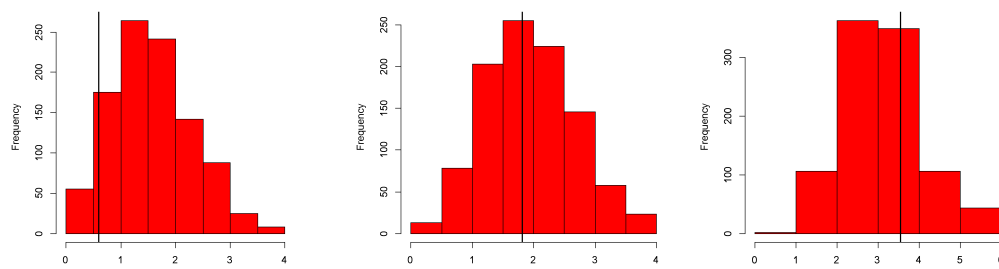


Figure 4 Posterior predictive distributions of the distance between final location of the track and point a with the vertical line indicating the observed value: Bioassay 1 (left panel), Bioassay 2 (middle panel) and Bioassay 3 (right panel).

small. As more data become available there will be the opportunity to extend the modelling to simultaneously model a large number of larvae tracks. However, we might expect to have to include in such models individual variation with regard to each larva. By increasing the sample size it will be possible to obtain a fuller understanding of the population behaviour of the larvae with regard to the attraction/repulsion.

Acknowledgements The authors would like to thank the Editor Dr. Lutz Edler, the Associate Editor and an anonymous referee for their extremely valuable comments and suggestions on an earlier version of this paper, which substantially improved the content and clarity of the article. We also thank Dr. Benjamin Hofner, the Reproducible Research Editor, for very helpful comments concerning the code. The experimental study was conducted at The James Hutton Institute, Invergowrie, Dundee. Chris McLellan is supported by an EPSRC studentship, and William Deasy is supported by an HDC studentship (FV 364 Novel approaches for the management of cabbage root fly).

Conflict of Interest

The authors have declared no conflict of interest.

References

- Anderson, T. W. (1971). *The Statistical Analysis of Time Series*. Wiley, New York.
- Blackwell, P. G. (1997). Random diffusion models for animal movement. *Ecological Modelling* **100**, 87–102.
- Blackwell, P. G. (2003). Bayesian inference for Markov processes with diffusion and discrete components. *Biometrika* **90**, 613–627.
- Box, G. E. P. and Tiao, G. C. (1973). *Bayesian Inference in Statistical Analysis*. Addison-Wesley, Reading, Massachusetts.
- Carlin, B. P. and Louis, T. A. (2008). *Bayesian Methods for Data Analysis*, Third Edition. Chapman and Hall/CRC, Boca Raton, Florida.
- Deasy, W. (2011). Novel approaches for the management of cabbage root fly. *Horticultural Development Company (HDC) Technical Seminar: Protecting Your Field Veg Crop*, 30th June 2011, Stockbridge Technology Centre, North Yorkshire, UK.
- Dunn, J. E. and Gipson, P. S. (1977). Analysis of radio telemetry data in studies of home range. *Biometrics* **33**, 85–101.
- Ewan, A. (2011). How to put root fly larvae off their food. *HDC News Field Vegetables Review*, Annual Supplement, Second Edition, 11.
- Finch, S. (1977). Effect of secondary plant substances on host-plant selection by the cabbage root fly. *Colloques Internationaux du Centre National de la Recherche Scientifique* **265**, 251–267.
- Frühwirth-Schnatter, S. (2006). *Finite Mixture and Markov Switching Models*. Springer, New York.

- Gelman, A., Carlin, J. B., Stern, H. S. and Rubin, D. B. (2003). *Bayesian Data Analysis*, Second Edition. Chapman and Hall/CRC, Boca Raton, Florida.
- Harris, K. J. and Blackwell, P. G. (2013). Flexible continuous-time modelling for heterogeneous animal movement. *Ecological Modelling* **255**, 29–37.
- Johnson, S. N. and Gregory, P. J. (2006). Chemically-mediated host-plant location and selection by root-feeding insects. *Physiological Entomology* **31**, 1–13.
- Košťál, V. (1992). Orientation behavior of newly hatched larvae of the cabbage maggot, *Delia radicum* (L.) (Diptera: Anthomyiidae), to volatile plant metabolites. *Journal of Insect Behavior* **5**, 61–70.
- Leonard, T. and Hsu, J. S. J. (1999). *Bayesian Methods: An Analysis for Statisticians and Interdisciplinary Researchers*. Cambridge University Press, Cambridge.
- Lunn, D. J., Thomas, A., Best, N. and Spiegelhalter, D. (2000). WinBUGS — A Bayesian modelling framework: concepts, structure, and extensibility. *Statistics and Computing* **10**, 325–337.
- McClintock, B. T., King, R., Thomas, L., Matthiopoulos, J., McConnell, B. J. and Morales, J. M. (2012). A general discrete-time modeling framework for animal movement using multistate random walks. *Ecological Monographs* **82**, 335–349.
- Nations, C. S. and Anderson-Sprecher, R. C. (2006). Estimation of animal location from radio telemetry data with temporal dependencies. *Journal of Agricultural, Biological and Environmental Statistics* **11**, 87–105.
- Noldus, L. P. J. J., Spink, A. J. and Tegelenbosch, R. A. J. (2001). EthoVision: a versatile video tracking system for automation of behavioral experiments. *Behavior Research Methods, Instruments and Computers* **33**, 398–414.
- Press, S. J. (1982). *Applied Multivariate Analysis: Using Bayesian and Frequentist Methods of Inference*, Second Edition. Krieger, Malabar, Florida.
- Ross, K. T. A. and Anderson, M. (1992). Larval responses of three vegetable root fly pests of the genus *Delia* (Diptera: Anthomyiidae) to plant volatiles. *Bulletin of Entomological Research* **82**, 393–398.
- Stephens, M. (2000). Dealing with label switching in mixture models. *Journal of the Royal Statistical Society, Series B* **62**, 795–809.
- Worton, B. J. (1995). Modelling radio-tracking data. *Environmental and Ecological Statistics* **2**, 15–23.